ISSN 0020-1685, Inorganic Materials, 2021, Vol. 57, No. 2, pp. 136–141. © Pleiades Publishing, Ltd., 2021.
Russian Text © The Author(s), 2021, published in Neorganicheskie Materialy, 2021, Vol. 57, No. 2, pp. 144–149.

Synthesis of Graphitic Carbon Nitride on the Surface of Fe_3O_4 Nanoparticles

E. B. Chubenko[a, *], A. V. Baglov[a], Yu. A. Fedotova[b], and V. E. Borisenko[a, c]

[a] *Belarussian State University of Informatics and Radio Engineering, Minsk, 220013 Belarus*
[b] *Institute for Nuclear Problems, Belarussian State University, Minsk, 220006 Belarus*
[c] *Moscow Engineering Physics Institute (National Nuclear Research University), Moscow, 115409 Russia*
**e-mail: eugene.chubenko@gmail.com*

Received April 13, 2020; revised September 23, 2020; accepted October 12, 2020

Abstract—A composite material consisting of graphitic carbon nitride and iron(II,III) oxide (g-C_3N_4/Fe_3O_4) and having photocatalytic and magnetic properties has been synthesized via single-step thermal decomposition of melamine in the presence of Fe_3O_4 nanoparticles. It has been shown that, at synthesis temperatures in the range 400–500°C, Fe^{2+} ions do not oxidize, and the Fe_3O_4 particles retain their crystal structure and ferromagnetic properties, but the process involves the formation of crystalline g-C_3N_4 as well. The maximum in the intensity of photoluminescence bands of the g-C_3N_4/Fe_3O_4 composite material is shifted to lower photon energies compared to g-C_3N_4 prepared without Fe_3O_4 particles under the same synthesis conditions, which is due to a decrease in its band gap, formed by a system consisting of C–N π bonds with sp^2 hybridization. The magnetic properties of g-C_3N_4/Fe_3O_4 composite particles allow them to be readily recovered from liquids for reuse.

Keywords: graphitic carbon nitride, iron(II,III) oxide, nanoparticles, X-ray diffractometry, photoluminescence

DOI: 10.1134/S0020168521020059

INTRODUCTION

At present, there is intensive research effort concentrated on a variety of materials for the fabrication of effective photocatalytic coatings suitable for use in systems for the removal of organic contamination from water and for hydrogen fuel generation [1]. Of particular interest among them is graphitic carbon nitride (g-C_3N_4), a polymeric organic semiconductor possessing high thermal stability (up to 600–650°C), chemical stability in alkaline and acid media, and attractive photocatalytic and photoluminescent properties [2, 3]. The optical band gap of g-C_3N_4 (2.70–2.88 eV at 300 K) is responsible for its rather high photocatalytic activity under illumination with solar light [2, 3]. The unique combination of its physical and optical properties makes it possible to employ g-C_3N_4 in light-emitting devices, chemical and biological sensors, and information display devices [2].

g-C_3N_4 is usually prepared via the pyrolytic decomposition of various nitrogen-containing organic substances, such as melamine, thiourea, urea, cyanamide, and dicyanamide, followed by thermal condensation and polymerization [2–4]. This method is incapable of producing a fully polymerized material because of the constant carbon loss during the synthesis process as a consequence of the formation of volatile carbon-containing compounds [5]. At the same time, it is defects on the surface of g-C_3N_4 which act as photocatalytic reaction centers, improving the efficiency of partially polymerized g-C_3N_4 compared to materials with a perfect crystal lattice [6, 7]. Since defects in materials are a parameter that is rather difficult to control, to modify and improve the properties of g-C_3N_4 a large number of g-C_3N_4-based heterosystems have been produced and investigated, including a variety of metals, semiconductors, and organic compounds [2, 8].

Iron(II,III) oxide (Fe_3O_4) is thought to be a potentially attractive component for the fabrication of g-C_3N_4-based heterostructures [9, 10]. Combining the Fe_3O_4 ferromagnet with g-C_3N_4 allows one to prevent agglomeration of g-C_3N_4 particles and improve photocatalysis efficiency owing to the formation of a heterogeneous system comprising a wide-band-gap organic semiconductor and a narrow-band-gap oxide semiconductor (half-metal). At present, such systems are typically produced using g-C_3N_4 ground into nanoparticles, with Fe_3O_4 particles grown on its surface by a hydrothermal process [9, 10]. This approach makes it possible to obtain a suspension of free

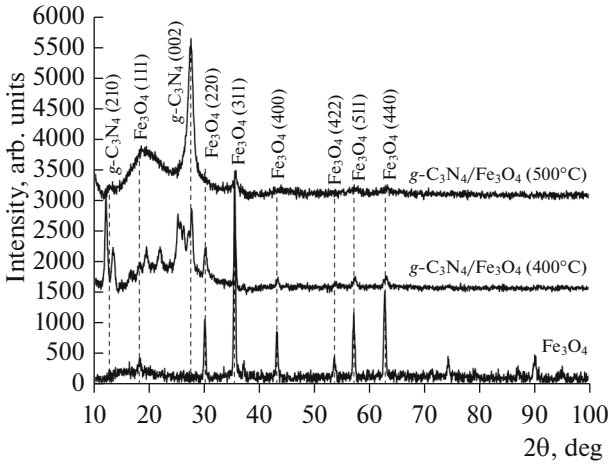

Fig. 1. X-ray diffraction patterns of the composite materials obtained at different synthesis temperatures.

Fe_3O_4/g-C_3N_4 nanoheteroparticles, which can readily be removed from the solution by a magnetic field after photocatalytic reaction [9, 10].

The purpose of this work was to investigate a new approach to the synthesis of g-C_3N_4/Fe_3O_4 heterostructures by an alternative method involving g-C_3N_4 formation on the surface of preprepared Fe_3O_4 nanoparticles via the pyrolytic decomposition of melamine at a temperature from 400 to 500°C in a single-step process, which made it possible to obtain a material structure "inverse" to a conventional one: with a Fe_3O_4 core coated with g-C_3N_4.

EXPERIMENTAL

The g-C_3N_4/Fe_3O_4 composite material was synthesized via the pyrolytic decomposition of starting reagents, followed by the polymerization of the reaction products in a closed atmosphere as described in previous reports [11, 12]. The starting reagents used were melamine and Fe_3O_4 powder (Sigma-Aldrich) consisting of spherical particles 50 to 100 nm in size. Before experiments, the melamine was ground in an agate mortar and mixed with Fe_3O_4 particles in the weight ratio 1 : 1. The resultant mixture (2 g), enclosed in a hermetically sealed 20-mL ceramic crucible, was placed in a muffle furnace and then heat-treated between 400 and 500°C for 30 min. The heating rate was 5°C/min. After the synthesis, the crucible was cooled over a period of up to 12 h.

The structure and composition of the synthesized material were determined by X-ray diffraction (DRON-3 diffractometer, CuK_α radiation, λ = 1.54179 Å) and X-ray photoelectron spectroscopy (Thermo Fisher ESCALAB 250Xi spectrometer). Photoluminescence spectra were obtained using a measuring system built around a Solar TII MS 7504i monochromator/spectrograph equipped with a Hamamatsu S7031-1006S Peltier-cooled CCD array digital camera. Photoluminescence was excited by a 1-kW xenon lamp. Monochromatic lines from the broad spectrum of the lamp were isolated using a Solar TII DM 160 double monochromator. The excitation wavelength was 345 nm. Photocatalytic activity of the synthesized material was characterized by the degree of decomposition of Rhodamine B model dye using a procedure described elsewhere [13].

RESULTS AND DISCUSSION

X-ray diffraction patterns of the synthesized material (Fig. 1) contain the 111, 220, 422, 511, and 440 lines of Fe_3O_4 and the 210 and 002 lines of g-C_3N_4 with a structure based on heptazine rings. There is also evidence for the presence of intermediate melamine decomposition and g-C_3N_4 polymerization reaction products: melem and melon [6, 14]. As the synthesis temperature is raised from 400 to 500°C, the lines related to g-C_3N_4 become sharper. In addition, they shift to smaller 2θ scattering angles. The [002] direction corresponds to the interplanar spacing between the carbon nitride sheets of monomolecular thickness, consisting of heptazine rings linked to each other.

The lattice parameters of g-C_3N_4 evaluated from the measured angular positions of its lines are a = 3.21 and 3.22 Å for the samples prepared at 400 and 500°C, respectively. The spacing between the linked triple aromatic rings of the heptazine units within one monomolecular g-C_3N_4 layer, as determined from the position of the 210 reflection from g-C_3N_4, is c = 6.51 and 6.83 Å at the same synthesis temperatures, and the average crystallite size evaluated from these data is 125 and 70 nm.

The intensity of the reflections from Fe_3O_4 in the X-ray diffraction pattern of the composite sample prepared at a temperature of 500°C is lower, but they still remain noticeable. At this temperature, the oxidation of the Fe^{2+} ions in the composition of the Fe_3O_4 particles to Fe^{3+}, resulting in Fe_2O_3 formation, is already possible, but the presence of lines corresponding to Fe_3O_4 suggests that this process does not occur under the conditions used in this study to synthesize the g-C_3N_4/Fe_3O_4 composite material.

The composition of the samples was determined by X-ray photoelectron spectroscopy, which showed the presence of nitrogen (46.68 at %), carbon (45.58 at %), oxygen (6.72 at %), and iron (1.02 at %), corresponding to g-C_3N_4 and Fe_3O_4 (Fig. 2). The quantitative atomic ratio is C : N = 0.98, exceeding the stoichiometric ratio (0.75) and suggesting that there is excess carbon in the material. The oxygen to iron atomic ratio

in the film is Fe : O = 0.15. The large deviation from the stoichiometric oxygen content of the iron oxide is related to the possibility of excess oxygen capture upon the formation of carbon nitride in the form of hydroxyl groups or to C–O bond formation [12]. The decomposition of a normalized portion of the spectrum with a band corresponding to the C 1*s* electron shell of carbon into symmetric Gaussians indicated the presence of individual bands at binding energies of 284.47, 287.08, and 287.97 eV (Fig. 3a). They are due to the presence of C=C double carbon bonds with sp^2 hybridization, C–O oxygen bonds, and N–C=N nitrogen bonds with sp^2 hybridization [15].

The asymmetric individual band corresponding to N 1*s* nitrogen bonds consists of three main lines, which are due to C–N=C carbon bonds (398.4 eV), $N-(C)_3$ nitrogen atoms coordinated by three carbon atoms (400 eV), and residual amine groups (401.2 eV) (Fig. 3b) [15]. Analysis of the O 1*s* line of the structures obtained in this study indicated the presence of oxygen–iron bonds (527.08 and 529.12 eV) [16, 17], O=O oxygen bonds (530.26 eV), N–C–O groups (531.83 eV), and oxygen or water adsorbed on the surface (534.6 eV) [15] (Fig. 3c).

In the binding energy range corresponding to Fe 2*p* shell electrons, there is a group of lines related to Fe(II) and Fe(III) ions [17]. The Fe 2*p* band is split into two components, $2p_{3/2}$ and $2p_{1/2}$, each having a satellite band. The $2p_{3/2}$ band can be decomposed into two components, corresponding to the Fe^{2+} $2p_{3/2}$ and Fe^{3+} $2p_{3/2}$ levels, at binding energies of 710.22 and 711.72 eV. The $2p_{1/2}$ band comprises two components, Fe^{2+} $2p_{1/2}$ and Fe^{3+} $2p_{1/2}$, at binding energies of 723.35 and 725.71 eV. The Fe^{2+} : Fe^{3+} ratio evaluated using the $2p_{3/2}$ band is 0.4, approaching that characteristic of stoichiometric Fe_3O_4. The $2p_{3/2}$: $2p_{1/2}$ ratio is 2.05, which also corresponds to that of stoichiometric Fe_3O_4 (2) [17].

The peak in the photoluminescence spectrum of the composite material prepared at a temperature of 500°C is located at a lower photon energy than is the peak in the spectrum of the material prepared at 400°C (Fig. 4).

The peak in the photoluminescence spectrum of the g-C_3N_4/Fe_3O_4 sample prepared at 400°C is located near 2.89 eV (Fig. 4, band I). The photoluminescence spectrum of the sample prepared at 500°C can be decomposed into two distinct bands (II and III), peaking near 2.80 and 2.68 eV, and its intensity is lower by a factor of 3. Comparison of the photoluminescence spectra of the composite materials with the spectra of g-C_3N_4 obtained at the same synthesis temperatures shows that the spectra of the composite materials are shifted to lower photon energies by 0.04–0.05 eV relative to those of g-C_3N_4. Note also that the

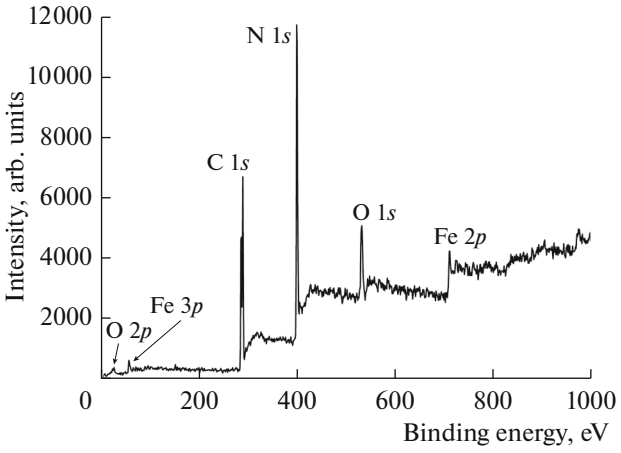

Fig. 2. Survey X-ray photoelectron spectroscopy scan of the g-C_3N_4/Fe_3O_4 composite material synthesized at 500°C.

spectrum of pure g-C_3N_4 prepared at a temperature of 500°C has no well-defined individual bands in the region of the peak.

The synthesized composite was found to exhibit photocatalytic activity comparable to that of pure g-C_3N_4. After exposure to light for 2 h, we observed essentially complete decoloration of a suspension containing Rhodamine B dye. In the dark, no decoloration of the suspension was detected. The presence of magnetic particles in the composite made it possible to increase the sedimentation rate when the suspension was placed in a static magnetic field. This allows the photocatalyst to be effectively recovered from purified solutions for reuse.

The present X-ray diffractometry and X-ray photoelectron spectroscopy results demonstrate that the synthesized composite material consists of g-C_3N_4 and crystalline Fe_3O_4. At the same time, the composite obtained at a synthesis temperature of 400°C contains a rather large amount of intermediate g-C_3N_4 formation reaction products, whose reflections are present in the X-ray diffraction patterns, suggesting that the polymerization of the melamine decomposition products did not reach completion. The lattice parameters of the g-C_3N_4 in this composite ($a_{400°C}$ = 3.21 Å and $c_{400°C}$ = 6.51 Å) differ drastically from those of completely polymerized, perfect g-C_3N_4 (a = 3.40 Å and c = 7.30 Å [5]), which also points to lattice distortions related to errors in the arrangement of the heptazine units in the g-C_3N_4 material.

The set of lines in X-ray diffraction patterns corresponding to Fe compounds shows that only crystalline Fe_3O_4 is present; that is, at the temperature under consideration there is no oxidation of Fe^{2+} ions to Fe^{3+}. The peak in the photoluminescence spectrum of the

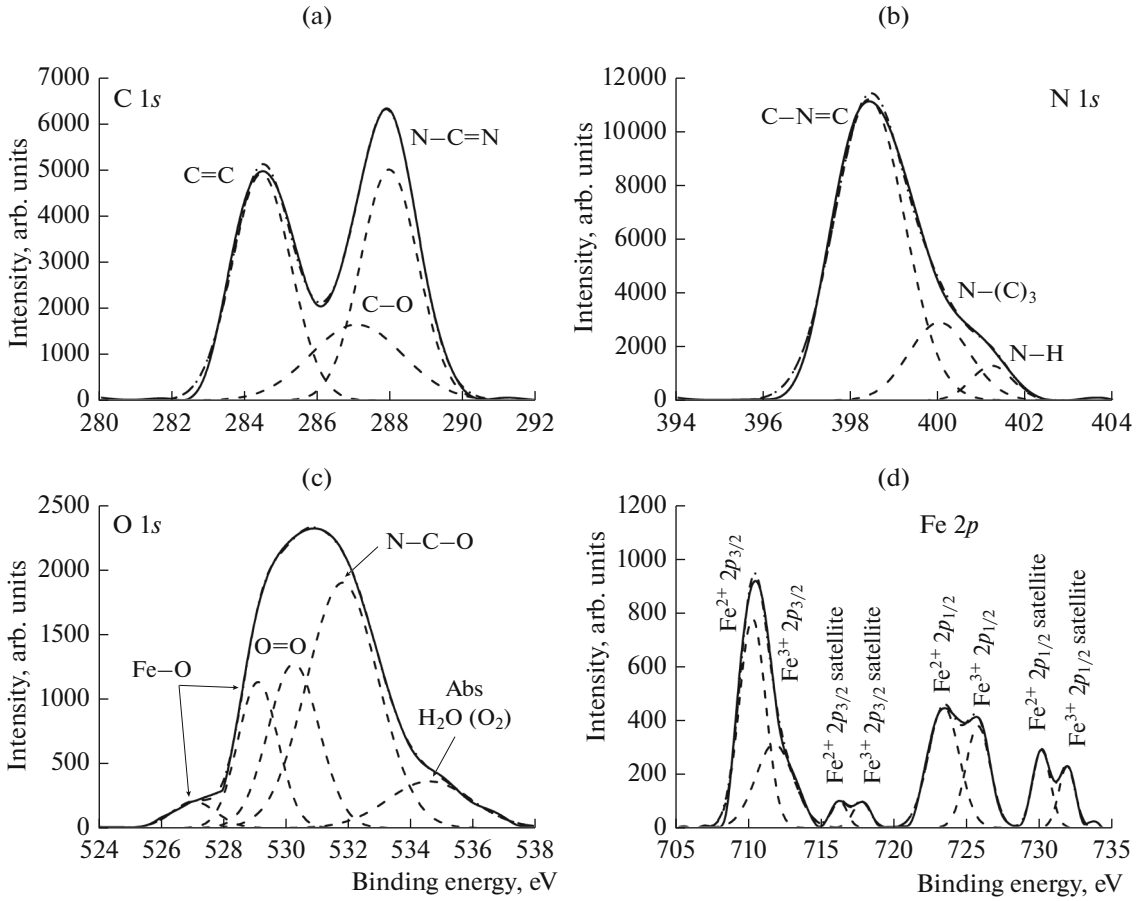

Fig. 3. X-ray photoelectron spectroscopy scans of the composite material synthesized at 500°C.

composite synthesized at 400°C is located at a higher photon energy than that of the sample synthesized at 500°C; that is, the energy of radiative transitions corresponds to a wider band gap. This can be accounted for by the fact that the valence and conduction bands of g-C_3N_4 with a low degree of polymerization are formed by C–N σ-bonds with sp^3 hybridization and their excited states, respectively, which form a system with a wider band gap [18]. The main type of radiative transition in the g-C_3N_4/Fe_3O_4 composite is a transition from an excited state level of σ-bonds to lone electron pair levels of nitrogen.

The shift of the luminescence band to lower photon energies in the samples synthesized at 500°C is due to the higher degree of polymerization of the material that has an increased number of C–N π-bonds with sp^2 hybridization, which form a structure characterized by a narrower band gap [18]. According to the present X-ray diffractometry data, the lattice parameters of the g-C_3N_4 obtained at this synthesis temperature approach those of a completely polymerized material. Incomplete polymerization is characteristic of g-C_3N_4 and is caused by so-called kinetic hindrances [9].

The present photoelectron spectroscopy results indicate the formation of carbon and nitrogen bonds characteristic of g-C_3N_4 [15] and demonstrate that the synthesized composite material contains an excess amount of oxygen, some of which is present in the g-C_3N_4 as well. Thus, the synthesized g-C_3N_4 can be thought of as doped with oxygen. The Fe^{2+} : Fe^{3+} ratio in the composite material synthesized at 500°C is also near that in stoichiometric Fe_3O_4, which means that we were able to avoid oxidation of Fe to Fe_2O_3 at this synthesis temperature. The presence of excess carbon in the synthesized structures is due to the decomposition of melamine and carbon-containing intermediate reaction products during the pyrolysis process and subsequent thermal polymerization.

In the photoluminescence spectrum of the material synthesized at 500°C, two bands can be distinguished, corresponding to transitions from excited π-bonds (Fig. 4, band II) and levels of lattice defects in the band gap (Fig. 4, band III) to a lone electron pair level of nitrogen atoms.

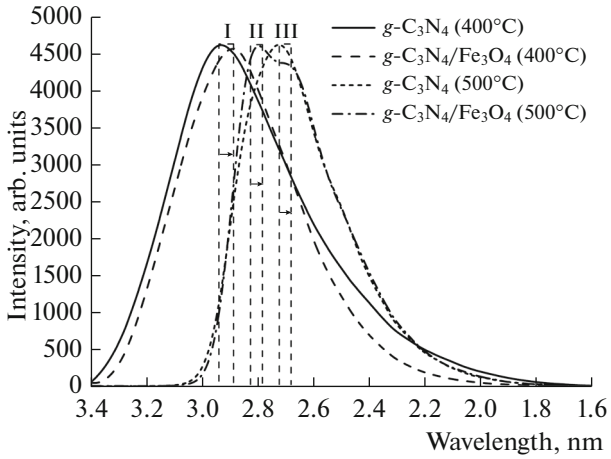

Fig. 4. Photoluminescence spectra of the g-C_3N_4 samples and composite materials synthesized at 400 and 500°C.

CONCLUSIONS

We have developed and investigated a simple, single-step process for the preparation of a g-C_3N_4/Fe_3O_4 composite material. Being comparable in photocatalytic activity to g-C_3N_4, this composite can be distributed in powder form over a liquid medium and, owing to the ferromagnetic properties of Fe_3O_4, can readily be recovered from such a suspension by an external magnetic field after use.

It has been shown that, at a synthesis temperature of 400°C, Fe_3O_4 nanoparticles have essentially no effect on g-C_3N_4 formation from melamine used as a starting reagent, even though the synthesized material contains its incomplete polymerization products. Synthesis at a temperature of 500°C ensures a more complete g-C_3N_4 polymerization.

In neither case was noticeable oxidation of Fe^{2+} ions in the Fe_3O_4 to Fe^{3+} detected. At the same time, photoluminescence spectra suggest that, at a synthesis temperature of 500°C, the presence of Fe_3O_4 nanoparticles in the starting mixture influences the structure of defects in g-C_3N_4, which is of considerable interest for the ability to control spectral characteristics of photo- and electroluminescent structures based on g-C_3N_4/Fe_3O_4 composites.

ACKNOWLEDGMENTS

We are grateful to Prof. V.V. Uglov for performing the X-ray diffraction characterizations of the samples and to Prof. X.W. Sun and Dr. M. Marus for analyzing the experimental samples by X-ray photoelectron spectroscopy.

FUNDING

This work was supported by the Belarussian Academy of Sciences and the Ministry of Education of the Republic of Belarus through the Materials Physics, Novel Materials, and Advanced Technologies National Research Program (task nos. 1.15 and 1.56).

V.E. Borisenko acknowledges the partial support of the Russian Federation Ministry of Science and Higher Education as part of the program aimed at improving the competitiveness of the Moscow Engineering Physics Institute (National Nuclear Research University).

REFERENCES

1. Spasiano, D., Marotta, R., Malato, S., Fernandez-Ibanez, P., and Di Somma, I., Solar photocatalysis: materials, reactors, some commercial, and pre-industrialized applications. A comprehensive approach, *Appl. Catal., B,* 2015, vol. 170, pp. 90–123.
2. Wang, A., Wang, C., Fu, L., Wong-Ng, W., and Lan, Y., Recent advances of graphitic carbon nitride-based structures and applications in catalyst, sensing, imaging, and LEDs, *Nano–Micro Lett.,* 2017, vol. 9, pp. 47–49.
3. Wen, J., Xie, J., Chen, X., and Li, X., A review on g-C_3N_4-based photocatalysts, *Appl. Surf. Sci.,* 2017, vol. 391, pp. 72–123.
4. Ong, W.-J., Tan, L.-L., Ng, Y.H., Yong, S.-T., and Chai, S.-P., Graphitic carbon nitride (g-C_3N_4)-based photocatalysts for artificial photosynthesis and environmental remediation: are we a step closer to achieving sustainability?, *Chem. Rev.,* 2016, vol. 116, pp. 7159–7329.
5. Fina, F., Callear, S.K., Carins, G.M., and Irvine, J.T.S., Structural investigation of graphitic carbon nitride via XRD and neutron diffraction, *Chem. Mater.,* 2015, vol. 27, pp. 2612–2618.
6. Thomas, A., Fischer, A., Goettmann, F., Antonietti, M., Müller, J.-O., Schlögl, R., and Carlsson, J.M., Graphitic carbon nitride materials: variation of structure and morphology and their use as metal-free catalysts, *J. Mater. Chem.,* 2008, vol. 18, pp. 4893–4908.
7. Wu, W., Zhang, J., Fan, W., Li, Z., Wang, L., Li, X., Wang, Y., Wang, R., Zheng, J., Wu, M., and Zeng, H., Remedying defects in carbon nitride to improve both photooxidation and H_2 generation efficiencies, *ACS Catal.,* 2016, vol. 6, pp. 3365–3371.
8. Sudhaik, A., Raizada, P., Shandilya, P., Jeong, D.-Y., Lim, J.-H., and Singh, P., Review on fabrication of graphitic carbon nitride based efficient nanocomposites for photodegradation of aqueous phase organic pollutants, *J. Ind. Eng. Chem.*, 2018, vol. 67, pp. 28–51.
9. Jia, X., Dai, R., Sun, Y., Song, H., and Wu, X., One-step hydrothermal synthesis of Fe_3O_4/g-C_3N_4 nanocomposites with improved photocatalytic activities, *J. Mater. Sci.: Mater. Electron.,* 2016, vol. 27, pp. 3791–3798.
10. Lima, M.J., Sampaio, M.J., Silva, C.G., Silva, A.M.T., and Faria, J.L., Magnetically recoverable Fe_3O_4/g-C_3N_4 composite for photocatalytic production of benzaldehyde under UV-LED radiation, *Catal. Today,* 2019, vol. 328, pp. 293–299.

11. Denisov, N.M., Chubenko, E.B., Bondarenko, V.P., and Borisenko, V.E., Synthesis of oxygen-doped graphitic carbon nitride from thiourea, *Tech. Phys Lett.,* 2019, vol. 45, pp. 108–110.

12. Chubenko, E.B., Baglov, A.V., Lisimova, E.S., and Borisenko, V.E., Synthesis of graphitic carbon nitride in porous silica glass, *Int. J. Nanosci.,* 2019, vol. 18, paper 1940042.

13. Denisov, N.M., Chubenko, E.B., Bondarenko, V.P., and Borisenko, V.E., Photoluminescence of ZnO/C nanocomposites formed by the sol–gel method, *J. Sol–Gel Sci. Technol.,* 2018, vol. 85, pp. 422–427.

14. Lotsch, B.V. and Schnick, W., New light on an old story: formation of melam during thermal condensation of melamine, *Chem. – Eur. J.,* 2007, vol. 13, pp. 4956–4969.

15. Kumar, R., Barakat, M.A., and Alseroury, F.A., Oxidized Fe_3O_4/*g*-C_3N_4/polyaniline nanofiber composite for the selective removal of hexavalent chromium, *Sci. Rep.,* 2017, vol. 7, paper 12850.

16. Geng, Z., Lin, Y., Yu, X., Shen, Q., Ma, L., Li, Z., Pan, N., and Wang, X., Highly efficient dye adsorption and removal: a functional hybrid of reduced graphene oxide–Fe_3O_4 nanoparticles as an easily regenerative adsorbent, *J. Mater. Chem.,* 2012, vol. 22, pp. 3527–3535.

17. Wilson, D. and Langell, M.A., XPS analysis of oleylamine/oleic acid capped Fe_3O_4 nanoparticles as a function of temperature, *Appl. Surf. Sci.,* 2014, vol. 303, pp. 6–13.

18. Jiang, Y., Sun, Z., Tang, C., Zhou, Y., Zeng, L., and Huang, L., Enhancement of photocatalytic hydrogen evolution activity of porous oxygen doped *g*-C_3N_4 with nitrogen defects induced by changing electron transition, *Appl. Catal., B,* 2019, vol. 240, pp. 30–38.

Translated by O. Tsarev